Author Manuscript

Author Manuscript

Author Manuscript

Author Manuscript

HHS Public Access

Author manuscript

Ann Otol Rhinol Laryngol. Author manuscript; available in PMC 2015 July 17.

Published in final edited form as:

Ann Otol Rhinol Laryngol. 2014 February ; 123(2): 124–134. doi:10.1177/0003489414523709.

Stem Cell–Derived Tissue–Engineered Constructs for Hemilaryngeal Reconstruction

Stacey L. Halum, MD, **Khadijeh Bijangi-Vishehsaraei, PhD**, **Hongji Zhang, MD**, **John Sowinski**, and **Marco C. Bottino, DDS, MSc, PhD**

Department of Otolaryngology–Head and Neck Surgery, Indiana University School of Medicine (Halum, Bijangi-Vishehsaraei, Zhang, Sowinski), and the Department of Restorative Dentistry/ Division of Dental Biomaterials, Indiana University School of Dentistry (Bottino). Indianapolis, Indiana

Abstract

Objectives—As an initial step toward our goal of developing a completely tissue-engineered larynx, the aim of this study was to describe and compare three strategies of creating tissue-engineered muscle-polymer constructs for hemilaryngeal reconstruction.

Methods—Cartilage-mimicking polymer was developed from electrospun poly(D,L-lactide-co-ε-caprolactone) (PCL). Primary muscle progenitor cell cultures were derived from syngeneic F344 rat skeletal muscle biopsies. Twenty F344 rats underwent resection of the outer hemilaryngeal cartilage with the underlying laryngeal adductor muscle. The defects were repaired with muscle stem cell–derived muscle–PCL constructs (5 animals), myotubc-derived muscle–PCL constructs (5 animals), motor end plate–expressing muscle–PCL constructs (5 animals), or PCL alone (controls; 5 animals). The outcome measures at 1 month included animal survival, muscle thickness, and innervation status as determined by electromyography and immunohistochemistry.

Results—All of the animals survived the 1-month implant period and had appropriate weight gain. The group that received motor end plate–expressing muscle–PCL constructs demonstrated the greatest muscle thickness and the strongest innervation, according to electromyographic activity and the percentage of motor end plates that had nerve contact.

Conclusions—Although all of the tissue-engineered constructs provided effective reconstruction, those that expressed motor end plates before implantation yielded muscle that was more strongly innervated and viable. This finding suggests that this novel approach may be useful in the development of a tissue-engineered laryngeal replacement.

Keywords

muscle progenitor cell; muscle stem cell; reconstruction; scaffold; tissue-engineered implant

Correspondence: Stacey L. Halum, MD, Dept of Otolaryngology–Head and Neck Surgery, 950 W Walnut St, Research II Building, E425, Indianapolis, IN 46202.

Drs Halum and Bijangi-Vishehsaraei contributed equally to the study.

Author Manuscript Author Manuscript Author Manuscript Author Manuscript

INTRODUCTION

Our ability to relay emotions, convey our personalities, and communicate effectively is intricately associated with our voicing ability. Neoplastic and traumatic injuries of the larynx can result in devastating voice impairment. Currently, laryngeal cancer affects more than 12,000 new individuals in the United States each year,[1] and many of those patients undergo partial laryngectomy or total laryngectomy with resultant sacrifice of voice quality. Iatrogenic traumatic avulsion of the vocal folds is another common source of irreversible vocal fold damage, with up to 6.3% of general anesthetic endotracheal intubations associated with traumatic injuries of the laryngopharynx.[2] Non-iatrogenic traumatic injury to the larynx is less common, affecting only 1 in 30,000 patients who present to the emergency department[3]; however, the injuries are often severe and likely to lead to permanent voice loss. These postoncologic or posttraumatic laryngeal injuries can be especially devastating to patients, because the lack of laryngeal airway protection and/or patency often renders the patients dependent on a gastrostomy and/or tracheostomy tube, in addition to causing them severe dysphonia.

To date, we have no clinically feasible options for replacing the larynx with a dynamic organ after neoplastic or traumatic partial or total laryngectomy. Microvascular or pedicled flaps are suboptimal reconstructive options for the vocal folds in that they require extensive surgery, involve donor site morbidity, and fail to restore dynamic motion. Although tissue-engineered muscle may be a future reconstructive option for the larynx, the literature suggests that inadequate innervation and muscle atrophy have been hurdles to this technology in other sites, such as the limbs.[4] No previous studies have investigated the innervation and posttransplant survival of tissue-engineered muscle used for muscle replacement in the larynx. In the knowledge that denervated laryngeal adductor muscles characteristically receive spontaneous reinnervation even after complete transection of the recurrent laryngeal nerve (RLN),[5–7] we hypothesized that tissue-engineered muscle would survive and become actively innervated when used for adductor muscle replacement in the larynx. In addition, evidence suggests that aneural motor end plates on myofibers in vivo will direct and promote axonal outgrowth to the aneural end plates and thereby lead to new neuromuscular junctions.[8] Thus, we hypothesized that tissue-engineered muscle-polymer implants that are created with motor end plate–expressing (MEE) myotubes (MTs) would result in enhanced innervation of the tissue-engineered muscle beyond that of muscle stem cell (MSC)–derived or MT-derived muscle–polymer implants alone. Specifically, the goal of this project was to test three different muscle-polymer implant construction strategies to determine whether one strategy would consistently provide a stable, nonimmunogenic, innervated tissue-engineered myochondral replacement for reconstruction of muscle and cartilage hemilaryngeal defects. This initial study is critical to our group's long-term goal of developing a completely tissue-engineered larynx for postlaryngectomy patients.

METHODS

TISSUE-ENGINEERED MUSCLE

Primary Muscle Progenitor Cell Cultures—Approximately 4 g of F344 rat skeletal muscle (see Animal Surgeries, below) was transferred to initial myogenic culture medium

Author Manuscript Author Manuscript Author Manuscript Author Manuscript

(IMCM) F-10 culture medium (Invitrogen, Life Technologies, Carlsbad, California; catalog number 11550–043) supplemented with 20% fetal bovine serum (HyClone Laboratories, Thermo Fisher Scientific, Waltham, Massachusetts; SH30070.03), 1% penicillin/streptomycin/amphotericin B (Cellgro; Mediatech, Inc, Manassas, Virginia; 30–004-CI), and 1% chicken embryo extract (SeraLab, Haywards Heath, England; CE-650-J). The muscle was minced into small pieces and digested in 0.2% collagenase type I (collagenase type 1–filtered; Worthington Biochemical Corp, Lakewood, New Jersey; LS004214) in IMCM within a shaking water bath at 37°C for 2 hours. The IMCM was added to digested muscle to terminate the reaction, and individual fibers were dissociated by rigorous pipetting. Digested tissue was filtered through a 300 μmol/L pore-size strainer and washed 3 times with IMCM. The pellet was resuspended in IMCM, and the muscle fibers were transferred into 3 wells of a 0.1% gelatin-coated 6-well culture plate (gelatin from porcine skin, type A; Sigma-Aldrich, St Louis, Missouri; G1890). Single fibers were confirmed by phase microscopy, and plates were left in a 5% carbon dioxide incubator at 37°C overnight. To prevent potential overgrowth of fibroblasts, we transferred the supernatant containing nonadhered muscle progenitor cells (MPCs) into 3 new wells of a 0.1% gelatin-coated 6-well plate after 24 hours. The medium was changed every other day. When primary cultures reached 70% confluency, they were passaged to prevent MT formation. The growth medium was changed to a myogenic culture medium (MCM; F-10 culture medium; Gibco, Grand Island. New York; 11550–043) supplemented with 10% fetal bovine serum (HyClone Laboratories; SH30070.03) and 1% penicillin/streptomycin (HyClone Laboratories; J110381) after the second passage. The MPCs, now in the form of MSCs (myoblasts and satellite cells) were maintained in 100-mm plates. MyoD expression and lack of MT-specific elongation confirmed a pure MSC population.

Strategies for Engineering Muscle-Polymer Implants In Vitro—Scaffolds of poly(D,L-lactide-co-ε-caprolactone) (PCL) were created as described in PCL Polymer Construction, below. Each scaffold was cut into 3 × 4-mm pieces and sterilized in 70% alcohol for 5 minutes. The scaffolds were rinsed in phosphate-buffered saline solution (PBS) and left under an ultraviolet light hood overnight for sterilization. Each PCL piece was seeded with approximately 8×10^5 MSCs within a 48-well plate in 300 μL MCM, and the plate was left on a rocker (Infinity Rocker; Nextadvance, Averill Park, New York) in a 37°C 5% carbon dioxide cell incubator for 1 hour of rocking at 15 cycles per minute. The seeding was repeated every day for 3 days. In the MSC group, cells were consistently passaged when the cell culture plate demonstrated 70% confluency, thereby preventing MT formation. In the MT group, the culture medium was switched to F10 supplemented with 10% horse serum on day 4 to induce MT formation. In the MEE group, the culture medium was supplemented with 10% horse serum to induce MT formation; in addition, our laboratory's optimized combination of additives to induce motor end plate expression, including acetylcholine chloride (Ach, 40 nmol/L; Tocris Bioscience, Bristol, England; 2809), agrin (10 nmol/L; R&D Systems, Minneapolis, Minnesota; 550-AG), and neuregulin (NRG1, 2 nmol/L; R&D Systems; 378-SM), was added to this medium, and the medium was changed every 3 days. Expression of motor end plates was confirmed with Alexa Fluor 594 conjugated α-bungarotoxin (Molecular Probes, Life Technologies; B13423; dilution 1:100) incubation for 1 hour, followed by visualization with the Olympus Flowviewer 1,000 mpe

Author Manuscript Author Manuscript Author Manuscript Author Manuscript

confocal/2-photon microscope (Fig 1). In all treatment groups, the muscle-polymer constructs were washed with PBS 6 days after varying the culture medium, and transferred to the animal operating room for implantation by sterile technique.

PCL POLYMER CONSTRUCTION

Scaffold Synthesis—The PCL (inherent viscosity, 1.29 dL g^{-1} in chloroform; Absorbable Polymers, Birmingham, Alabama) scaffolds were fabricated via electrospinning with use of a conventional setup comprising a high-voltage source (ES50P-10W/DAM; Gamma High Voltage Research, Ormond Beach, Florida), a syringe pump (Legato 200; KD Scientific, Holliston, Massachusetts), and a grounded stainless steel collecting mandrel as previously described.[9] In brief, the electrospinning processing parameters, including the solution concentration (10 to 20 wt% PCL) and the field strength (voltage), were optimized to achieve defect-free fibrous structures. Both the flow rate and the spinneret-to-collector distance were kept constant at 1 mL/h and 18 cm, respectively. The optimum defect-free and homogeneous fiber diameter scaffold was obtained by dissolving PCL in hexafluoroisopropanol (HFP; Sigma-Aldrich) overnight under stirring conditions at 150 mg/mL. The formulation was loaded in a plastic syringe fitted with a 27-gauge stainless needle and electrospun at 10 kV. The scaffolds were kept at room temperature for 2 days in a vacuum desiccator to remove any residual solvent.

Scaffold Characterization—Scanning electron microscopy (SEM; JSM-5310LV; JEOL, Tokyo, Japan) was used to assess fiber morphology and the overall scaffold porous structure that would facilitate myoblast or MT attachment. Briefly, small samples were excised from each of the scaffolds obtained in the optimization process. Then, samples were mounted on aluminum stubs, sputter-coated with gold, and imaged at 15 keV. The average fiber diameter was calculated from measurements obtained with Image J 1.40G software (US National Institutes of Health) on 3 distinct SEM images. Mechanical testing of the optimized scaffold (ie, PCL at 15 wt%) was performed by uni-axial microtensile testing (eXpert 5601; Admet, Norwood, Massachusetts) on rectangular samples (15 × 3 mm) at a cross-head speed of 5 mm/min. Similarly, the mechanical strength of the rat native laryngeal cartilage was also measured. The maximum load needed to produce fracture was recorded (N/mm^2 = MPa) on dedicated software. The results are reported as mean ± SD.

ANIMAL SURGERIES

The study protocol was approved by the Indiana School of Medicine Animal Care and Use Committee, and institutional guidelines, in accordance with the National Institutes of Health guidelines, were followed for the handling and care of the animals. Because Fischer 344 males are syngeneic, 1 donor animal was used to create tissue-engineered constructs for 20 study animals.

Muscle Harvest—One Fischer 344 male rat (Harlan Laboratories, Indianapolis, Indiana) was anesthetized with intraperitoneal administration of ketamine hydrochloride (75 mg/kg) and xylazine hydrochloride (10 mg/kg), and a 1-cm vertical cervical incision was created at midline. Dissection proceeded to the cervical muscles, and approximately 4 g of cervical muscle (strap and sternocleidomastoid muscles) was harvested and placed immediately in

Author Manuscript Author Manuscript Author Manuscript Author Manuscript

IMCM. The steps outlined in Primary Muscle Progenitor Cell Cultures, above, were then followed.

Partial Laryngectomy Procedures—Twenty Fischer 344 male rats (Harlan Laboratories) were anesthetized with intraperitoneal administration of ketamine hydrochloride (75 mg/kg) and xylazine hydrochloride (10 mg/kg), and underwent resection of the left lateral thyroid cartilage with as much adductor muscle (lateral and medial thyroarytenoid, alar cricoarytenoid, and lateral cricoarytenoid) as could be safely removed without violation of the inner mucosa. Mucosal violation was avoided to minimize infection risk. Animals were randomized to undergo repair with PCL polymer scaffolds alone (5 animals; control or PCL group), MSC-based muscle–polymer constructs (5 animals; MSC group), MT-based muscle–polymer constructs (5 animals; MT group), or MEE muscle–polymer constructs (5 animals; MEE group; Fig 2). After the implant was secured, the strap muscles were reapproximated and the skin was closed with 5-0 Vicryl suture.

Evaluation Under Anesthesia—After 1 month, the animals were returned to the operating room to be placed under anesthesia with inhalational isoflurane, which was titrated to permit stimulation-induced laryngospasm. Under anesthesia, laryngeal electromyography (LEMG; Niking Viking Quest electromyography machine, Madison, Wisconsin) was used to test the adductor muscle complex and the posterior cricoarytenoid (PCA) muscles bilaterally with a 25-gauge bipolar concentric needle, with use of an amplitude of 50 to 100 μV, 10- to 100-ms sweep speeds, and a clamp on exposed lateral neck muscle for grounding. To ensure optimal needle insertion, we created a neck incision and exposed the larynx to allow direct visualization of the implant and laryngeal anatomy during the LEMG. Needle insertion into the PCA muscle was done directly while the larynx was gently rotated contralaterally. The adductor complex was tested via the cricothyroid membrane. The PCA and adductor muscles were tested first so that firing patterns in the engineered muscle could be assessed relative to the native laryngeal muscles. To determine whether the tissue-engineered muscle constructs were firing congruently with native adductor and/or PCA muscles, we performed LEMG at 100 μV and 100-ms sweep speeds, and captured patterns of firing from the tissue-engineered muscle and compared them to those from the adductor complex and the PCA muscle. The PCA muscle's highly characteristic inspiratory bursts of activity (Fig 3F) allowed tracings to be directly compared and inspiratory firing to be readily identified. The tissue-engineered muscle was tested by inserting the needle into the luminal side of the implant and identifying crisp areas of signaling while maintaining contact with the polymer. Qualitative comparison of recruitment was done during laryngospasm at 50 μV and 10-ms sweep. As the isoflurane anesthesia was lightened (by lowering the percentage of isoflurane), the animals went into laryngospasm as a 25-gauge needle was inserted via the cricothyroid membrane into the laryngeal airway. The LEMG needle was inserted into the muscle of interest to obtain a recording, and the isoflurane levels were then increased again to deepen the animals' anesthesia. After the LEMG was completed, the animal was placed under deeper anesthesia with intraperitoneal administration of ketamine hydrochloride (75 mg/kg) and xylazine hydrochloride (10 mg/kg) and euthanized. The larynx, implant, and strap muscles overlying the implant were harvested en bloc for further analysis.

Author Manuscript Author Manuscript Author Manuscript Author Manuscript

IMMUNOHISTOCHEMISTRY

Percentage of Motor End Plates With Neuronal Contact—After harvested specimens were incubated for a 12-hour period with 4% paraformaldehyde at 4°C, they were transferred into 30% sucrose at 4°C for an additional 24 hours. Axial cryosectioning was performed with 12-μm thickness on 3% gelatin-coated slides. The cryosections were washed in PBS 3 times. They were incubated in 0.3 mol/L glycine in PBS for 20 minutes. The sections were then permeabilized in 0.1% Triton X-100 in PBS for 20 minutes. They were washed with PBS 3 times and then blocked with 4% goat serum for 1 hour. After an overnight incubation at 4°C with rabbit polyclonal class III β-tubulin (Covance, Richmond, California; PRB-435p) at 1/1,000 dilution, slides were incubated with Alexa Fluor 488 conjugated goat anti-rabbit immunoglobulin G secondary antibody (Invitrogen; A11034) for 1 hour. To visualize the motor end plates in the same sections, we incubated them with Alexa Fluor 594 conjugated α-bungarotoxin (Molecular Probes; B13423; dilution 1:100) for 1 hour. The sections were observed with the Olympus Flowviewer 1,000 mpe confocal/2-photon microscope.

Assessment of Rejection Markers—Specimen fixation and cryosectioning were performed as described in the preceding paragraph. The sections were hydrated by 2 changes of PBS. The slides were immersed in Liberate Antibody Binding (LAB) epitope retrieval solution (Polysciences, Inc, Warrington, Pennsylvania; 24310) for 15 minutes, and then endogenous peroxidase was inactivated by incubation with 3% hydrogen peroxide (Sigma-A1-drich; H1009) in methanol for 5 minutes. To block nonspecific binding sites, we incubated the sections with 1.5% normal horse serum (Vectastain ABC kit; mouse immunoglobulin G; Vector Laboratories, Burlingame, California; PK-6102) in a humidification chamber for 30 minutes. The sections were incubated with monoclonal antibodies overnight at 4°C at 1:50 dilution: mouse anti-CD3 antibody (Abcam, Cambridge, Massachusetts; B355.1; ab8671), mouse anti-CD4 antibody (Abcam; CA-4; ab82252), and mouse anti-CD8a antibody (BD Biosciences, San Jose, California; 554854). After being washed 3 times with PBS, the sections were incubated with anti-mouse biotinylated secondary antibody for 30 minutes at room temperature. After being washed twice with PBS, the sections were incubated with Vectastain Elite ABC reagent (Vectastain ABC kit; mouse immunoglobulin G; Vector Laboratories, PK-6102) for 30 minutes at room temperature. After washings with 2 changes of PBS, the sections were incubated with peroxidase substrate solution (chromogenic substrate 3,3′-diaminobenzidine tetrahydrochloride; Sigma-Aldrich; D5905) for 1 minute. The sections were then counterstained in modified Harris hematoxylin (Richard-Allan Scientific, Thermo Fisher Scientific; 72704) for 1 minute before dehydration and mounting (Eukitt; Election Microscopy Sciences, Hatfield, Pennsylvania; 15322).

MUSCLE THICKNESS

Specimen fixation and cryosectioning were performed as described above, in the first paragraph of Immunohistochemistry. For each animal, 6 axial sections of 12-μm thickness were created through the mid-portion of the implant to be used for hematoxylin-eosin staining. The sections were rehydrated for 1 minute in water followed by 1 minute of staining with modified Harris hematoxylin and 1 minute of staining with 0.25% eosin

Author Manuscript Author Manuscript Author Manuscript Author Manuscript

(Fisher Scientific; SE22-500D). The sections were dehydrated with alcohol, cleared with xylenes, and mounted by Eukitt. The slides were then assessed under microscopy, and images were captured of the slides that demonstrated the maximal muscle-polymer thickness for each animal. Image J was used to measure the thickness of the tissue-engineered muscle on the surface of each implant at 3 sites, and the average maximum muscle thickness and mean thickness were then calculated for each specimen.

STATISTICAL ANALYSIS

Student's *t*-test was used to compare changes in the treatment groups to those in the control group. Analysis of variance was used to compare differences between treatment groups. For all statistical tests, significance was set at a p level of less than 0.05.

RESULTS

SCAFFOLD CHARACTERIZATION

Figure 4A–F shows representative SEM images of nonoptimized electrospun PCL fibers at different processing parameters. The mean fiber diameter was strongly dependent on the processing conditions used. The nonoptimized electrospun mean fiber diameters ranged from 645 nm to 3.9 μm. Specifically, we observed that increasing both the polymer solution concentration and the field strength (voltage) led to an increase in fiber diameter. More important, even though PCL at 150 mg/mL yielded thicker fibers than did the 100 mg/mL solution at the same voltage (645 ± 641 nm), a narrower fiber distribution was seen in this optimized condition (1.62 ± 0.41 μm). Furthermore, all of the different scaffolds revealed an open porosity and an interconnected structure; however, the SEM images for the optimized condition suggest larger pore sizes (approximately 15 to 20 μm), which in turn would allow for better cell infiltration. Thus, 15 wt% PCL with a voltage of 10 kV and a flow rate of 1 mL/h demonstrated the ideal scaffold characteristics (Fig. 4G,H), with porosity and fiber thickness that promote cellular and vascular ingrowth, and fiber diameters that provide adequate structural support for the hemilarynx. Table 1 shows the PCL scaffolds' mechanical data recorded before implantation, which demonstrated load tolerance and tensile strength similar to those of native rat cartilage.

ANIMAL SURGERIES

One animal in the MT group failed to awaken from the initial surgery because of anesthesia-related problems, and the remaining 19 animals survived. All surviving animals steadily gained weight in the postoperative period.

LEMG—At 1 month after implantation, LEMG demonstrated the most motor unit potentials in the MSC and MEE groups, demonstrated no activity in the PCL group, and demonstrated minimal activity in the MT group (Fig. 3). In all animals, the LEMG activity was synchronized with contralateral adductor muscle firing — a finding suggesting that the tissue-engineered muscle had received adductor innervation.

Percentage of Motor End Plates With Neuronal Contact—For each group, we analyzed 6 images of axial sections from each specimen and determined the percentage of

Author Manuscript Author Manuscript Author Manuscript Author Manuscript

motor end plates with nerve contact after counting a minimum of 150 end plates for each group. There were no motor end plates detected in the PCL group, whereas the other groups all demonstrated motor end plates (Fig. 5). The mean percentages of motor end plates with nerve contact were 82.4%, 65.8%, and 94.8% for the MSC group, the MT group, and the MEE group, respectively (Table 2).

Muscle Thickness—The tissue-engineered myofibers were characterized by a disorganized appearance that allowed the tissue-engineered muscle to be readily discerned from any residual native adductor muscle located deep to the implant (Fig. 6). The mean thicknesses from the inner border of the PCL implant to the outer border of the tissue-engineered muscle were 587.3 μm, 680.2 μm, and 750.3 μm for the MSC group, the MT group, and the MEE group, respectively (Table 2).

Assessment of Rejection Markers—Rejection markers failed to demonstrate immunorejection of any specimens, although a nonspecific inflammatory reaction could be detected around the implant in many sections (Fig. 7).

DISCUSSION

The goal of this project was to test three different muscle-polymer implant fabrication strategies to determine whether any approach could provide a stable, nonimmunogenic, innervated tissue-engineered replacement for reconstruction of muscle and cartilaginous hemilaryngeal defects. The tissue-engineered muscle in the MSC group was created from premature MPC subtypes consisting of satellite cells and myoblasts, in the MT group the muscle was derived from unmodified mature MPCs called MTs (multinucleated muscle cells), and in the MEE group the muscle was derived from MTs modified to express motor end plates.[10–12] We anticipated that a 1-month implantation period would be adequate to assess the innervation of the implants for two reasons: 1) spontaneous reinnervation in the rat occurs much earlier than that seen in humans in models of RLN injury,[7,13,14] and 2) since the RLN was not actually transected in this model, innervation of the muscle-polymer implants likely occurred via axonal spouting and regeneration of adductor RLN fibers injured during the myectomy procedure, and the close proximity of the regenerating axons and the tissue-engineered muscle likely facilitated rapid implant innervation. We hypothesized that the increased expression of motor end plates in the MEE group may lead to postmyectomy axonal sprouting and regeneration directed toward the aneural end plates, as occurs after acute denervation injury.[7] According to the percentage of motor end plates with nerve contact, the MEE group did demonstrate significantly greater innervation than did the other groups; nearly 95% of the end plates had nerve contact at just 1 month. The LEMG activity demonstrated bursts of motor unit potentials that fired in synchrony with the native adductor complex, suggesting that the muscle might have functional contraction if a more organized network of muscle were engineered. Interestingly, the MSC group also demonstrated a very high rate of innervation and a high prevalence of motor end plates within the myofibers, with more than 82% of motor end plates demonstrating neuronal contact. The primitive and reparative nature of the MSCs may have resulted in this innately strong tendency to develop neuromuscular junctions in vivo. However, MSCs are also characterized by their postimplantation differentiation and fusion to form MTs, which then

Author Manuscript Author Manuscript Author Manuscript Author Manuscript

fuse to form myofibers in vivo. As many MSCs (myoblasts) are required for the formation of a single multinucleated MT, it might be anticipated that the fusion process would lead to a loss of muscle volume when MSC-based constructs are implanted in vivo. Indeed, the postimplantation thickness of the tissue-engineered muscle was significantly lower in the MSC group than in the MT and MEE groups. For both of the MT-based groups (MT and MEE), the thickness of the muscle was closely associated with the innervation status of the engineered muscle. These findings suggest that tissue-engineered muscle thickness (survival) is directly dependent on innervation, and that atrophy will occur without innervation, just as atrophy occurs when innate myofibers become acutely denervated.[13,14]

The PCL scaffold in the current model displays clear advantages and disadvantages. The advantages of the PCL scaffold include its ability to be fabricated expediently in large quantities without any donor tissues (as required with alternatives such as decellularized cartilage), its ability to foster myogenic cell growth and adherence, and its stability after implantation. Among the disadvantages, there was evidence of a diffuse inflammatory infiltrate surrounding the PCL, likely mediating gradual bio-absorption of the implant, as is known to occur.[15] In addition, because the electrospun PCL scaffold provided the foundation for myogenic cell adhesion, the resultant tissue-engineered muscle displayed a multidirectional interwoven network similar to that of the underlying polymer. Because our future goal is to create a *functional* myochondral replacement, the muscle will need to be organized and unidirectional, and thus a scaffold material will need to be developed to better support the desired organization and directionality of the tissue-engineered muscle. Electrospinning techniques can be customized to create a uniform, striated inner scaffold surface that would likely improve the organization of the myofibers. To improve myofiber organization, our laboratory is not only further tailoring the fabrication process to yield nanosized and aligned fibers, but also investigating the use of decellularized larynges as a framework material for laryngeal tissue engineering. Future studies will incorporate stem cell–derived cartilage, muscle, and vibratory epithelium,[16,17] thus paving the way to our long-term goal of developing a completely tissue-engineered larynx.

CONCLUSIONS

The current study demonstrates that a tissue-engineered myopolymer implant derived from autologous MPCs can be used for myochondral hemilaryngectomy reconstruction. Furthermore, this report introduces a novel method of inducing expression of motor end plates on myogenic cells in vitro that results in a significant advance in the innervation and viability of tissue-engineered muscle. These experiments represent essential initial steps directing us toward our long-term goal of developing a functional tissue-engineered laryngeal replacement.

Acknowledgments

These projects were in part supported by award number K08DC009583 from the National Institute on Deafness and Other Communication Disorders (NIDCD) within the National Institutes of Health (NIH). These projects were supported in part by a Project Development Team within the ICTSI NIH/NCRR, grant TR000006. The content of this publication is solely the responsibility of the authors and does not necessarily represent the official views of the NIDCD or NIH. These projects were supported in part by an Indiana University Collaborative Research Grant. The projects were also in part supported by an award from the Indiana University School of Medicine Center for

Author Manuscript Author Manuscript Author Manuscript Author Manuscript

Translational Science Institute (CTSI). The authors completed these experiments in alignment with the ethical research guidelines of our institution and the NIH. This study was performed in accordance with the PHS Policy on Humane Care and Use of Laboratory Animals, the NIH *Guide for the Care and Use of Laboratory Animals*, and the Animal Welfare Act (7 U.S.C. et seq.); the animal use protocol was approved by the Institutional Animal Care and Use Committee (IACUC) of Indiana University.

References

1. American Cancer Society. Cancer Facts and Figures 2012. Atlanta, Ga: American Cancer Society; 2012.
2. Peppard SB, Dickens JH. Laryngeal injury following short-term intubation. Ann Otol Rhinol Laryngol. 1983; 92:327–30. [PubMed: 6881831]
3. Inagi K, Schultz E, Ford CN. An anatomic study of the rat larynx: establishing the rat model for neuromuscular function. Otolaryngol Head Neck Surg. 1998; 118:74–81. [PubMed: 9450832]
4. Kang S-B, Olson JL, Atala A, Yoo JJ. Functional recovery of completely denervated muscle: implications for innervation of tissue-engineered muscle. Tissue Eng Part A. 2012; 18:1912–20. [PubMed: 22559300]
5. Blitzer A, Jahn AF, Keidar A. Semon's law revisited: an electromyographic analysis of laryngeal synkinesis. Ann Otol Rhinol Laryngol. 1996; 105:764–9. [PubMed: 8865770]
6. Woodson GE. Spontaneous laryngeal reinnervation after recurrent laryngeal or vagus nerve injury. Ann Otol Rhinol Laryngol. 2007; 116:57–65. [PubMed: 17305279]
7. Hydman J, Mattsson P. Collateral reinnervation by the superior laryngeal nerve after recurrent laryngeal nerve injury. Muscle Nerve. 2008; 38:1280–9. [PubMed: 18816603]
8. Vock VM, Ponomareva ON, Rimer M. Evidence for muscle-dependent neuromuscular synaptic site determination in mammals. J Neurosci. 2008; 28:3123–30. [PubMed: 18354015]
9. Bottino MC, Thomas V, Janowski GM. A novel spatially designed and functionally graded electrospun membrane for periodontal regeneration. Acta Biomater. 2011; 7:216–24. [PubMed: 20801241]
10. Cohen I, Rimer M, Lømo T, McMahan UJ. Agrin-induced postsynaptic-like apparatus in skeletal muscle fibers in vivo. Mol Cell Neurosci. 1997; 9:237–53. [PubMed: 9268503]
11. Ngo ST, Cole RN, Sunn N, Phillips WD, Noakes PG. Neuregulin-1 potentiates agrin-induced acetylcholine receptor clustering through muscle-specific kinase phosphorylation. J Cell Sci. 2012; 125(Pt 6):1531–43. [PubMed: 22328506]
12. Jones G, Meier T, Lichtsteiner M, Witzemann V, Sakmann B, Brenner HR. Induction by agrin of ectopic and functional postsynaptic-like membrane in innervated muscle. Proc Natl Acad Sci U S A. 1997; 94:2654–9. [PubMed: 9122251]
13. Halum SL, Hiatt KK, Naidu M, Sufyan AS, Clapp DW. Optimization of autologous muscle stem cell survival in the denervated hemilarynx. Laryngoscope. 2008; 118:1308–12. [PubMed: 18401272]
14. Halum SL, Naidu M, Delo DM, Atala A, Hingtgen CM. Injection of autologous muscle stem cells (myoblasts) for the treatment of vocal fold paralysis: a pilot study. Laryngoscope. 2007; 117:917–22. [PubMed: 17473696]
15. Zhou WY, Guo B, Liu M, Liao R, Rabie ABM, Jia D. Poly(vinyl alcohol)/halloysite nanotubes bionanocomposite films: properties and in vitro osteoblasts and fibroblasts response. J Biomed Mater Res A. 2010; 93:1574–87. [PubMed: 20014291]
16. Long JL, Neubauer J, Zhang Z, Zuk P, Berke GS, Chhetri DK. Functional testing of a tissue-engineered vocal fold cover replacement. Otolaryngol Head Neck Surg. 2010; 142:438–40. [PubMed: 20172395]
17. Long JL, Zuk P, Berke GS, Chhetri DK. Epithelial differentiation of adipose-derived stem cells for laryngeal tissue engineering. Laryngoscope. 2010; 120:125–31. [PubMed: 19856398]

Author Manuscript Author Manuscript Author Manuscript Author Manuscript

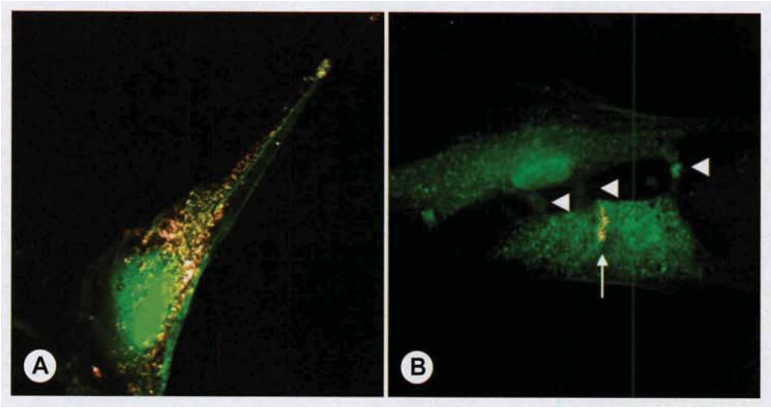

Fig 1.

Motor end plate formation in culture. For in vitro visualization, muscle progenitor cells in this Figure are expressing enhanced green fluorescent protein (EGFP: green), although tissue-engineered muscle-polymer implants used for implantation were created with unmodified primary muscle stem cells (MSCs). **A**) When primary cultures were passaged to prevent myotube (MT) differentiation (as described in Primary Muscle Progenitor Cell Cultures section) and incubated with acetylcholine, agrin, and neuregulin, α-bungarotoxin staining depicted expression of acetylcholine receptors (AChRs) on individual MSC surface (gray). **B**) To induce multinucleated MT formation (as described for MT group, ie, group with MT-derived muscle–PCL [poly(D,L-lactide-co-ε-caprolactone)] constructs), we incubated cells in nutrient-poor microenvironment (10% horse serum) that induced myoblasts to fuse with one another (arrowheads demarcating contact points between fusing myoblasts). In MEE group (group with motor end plate–expressing muscle–PCL constructs), cells were incubated in MT medium with acetylcholine, agrin, and neuregulin (as described in Methods) to induce AChR formation. Note that whereas AChRs formed on the MSC surface (in **A**), developing MTs formed mature motor end plates (arrow).

Author Manuscript Author Manuscript Author Manuscript Author Manuscript

Fig 2.

Intraoperative implant positioning. Left hemilaryngeal cartilage with underlying adductor muscle has been resected, with care taken to avoid intralaryngeal mucosal violation. Implant (black arrow) is secured with tissue-engineered muscle facing inward and outer PCL scaffold adjacent to native right hemilaryngeal cartilage (white solid arrow). PCL scaffold is slightly oversized to overlap cricothyroid membrane above cricoid cartilage (white dotted arrow).

Author Manuscript Author Manuscript Author Manuscript Author Manuscript

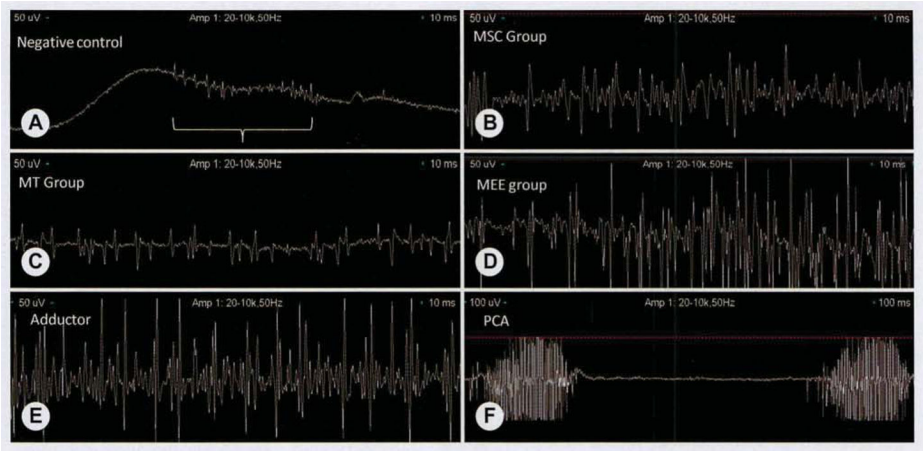

Fig 3.

Representative laryngeal electromyography (EMG) findings. To detect relative differences in activity levels, we recorded laryngeal EMG tracings with amplitude of 50 μV and sweep speed of 10 ms (**A–E**). To demonstrate inspiratory firing of posterior cricoarytenoid (PCA) muscle, we recorded tracing at amplitude of 50 μV and sweep speed of 100 ms (**F**). **A**) In negative PCL control, no active motor unit potentials were detected because of absence of significant tissue-engineered muscle on implant. Fact that insertional activity was reproducible (bracket) when EMG recording needle was inserted directly into PCL implant suggests that sparsely populated noninnervated muscle cells had infiltrated scaffold. **B**) MSC group (group with MSC-based muscle–polymer constructs) demonstrated low levels of motor unit potentials that fired in synchrony with contralateral adductor muscle during laryngospasm. No inspiratory firing was noted. **C**) MT group (see Fig 1 for definition) demonstrated qualitatively less recruitment upon laryngospasm, and as in MSC group, there were no inspiratory bursts of activity. **D**) MEE group (see Fig 1 for definition) demonstrated bursts of motor unit potentials that were firing with intensity and timing similar to those of contralateral native adductor muscle complex. As in MSC and MT groups, no inspiratory firing was detected. **E**) Native adductor muscle complex demonstrated bursts of motor unit potentials during laryngospasm and no active firing on inspiration. **F**) Although relative degree of recruitment did not differ significantly between adductor complex and PCA muscle, PCA muscle demonstrated characteristic inspiratory bursts of activity that were absent in native adductor complex and tissue-engineered muscle.

Author Manuscript Author Manuscript Author Manuscript Author Manuscript

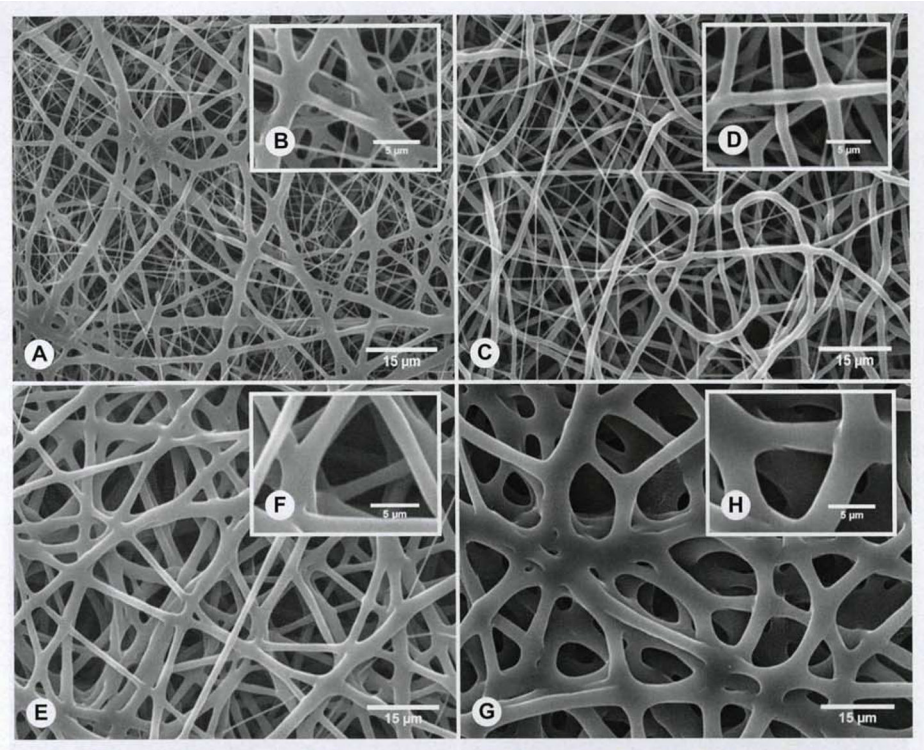

Fig. 4.

PCL implants electrospun with different porosities. **A–H**) Representative scanning electron microscopy (SEM) images of electrospun fibers obtained during optimization process. **A,B**) PCL fibers obtained from 100 mg/mL solution with electrospinning parameters 10 kV, 18 cm, and 1 mL/h. **C,D**) PCL fibers obtained from 100 mg/mL solution with electrospinning parameters 18 kV, 18 cm, and 1 mL/h. **E,F**) PCL fibers obtained from 200 mg/mL solution with electrospinning parameters 18 kV, 18 cm, and 1 mL/h. **G,H**) Representative SEM images of optimized PCL fibers obtained from 150 mg/mL solution with electrospinning parameters 10 kV, 18 cm, and 1 mL/h. Note larger open pores and more homogeneous fiber diameter at these processing parameters in comparison to other, nonoptimal conditions (**A–F**). Insets (**B,D,F,H**) show higher-magnification images (5,000×).

Author Manuscript Author Manuscript Author Manuscript Author Manuscript

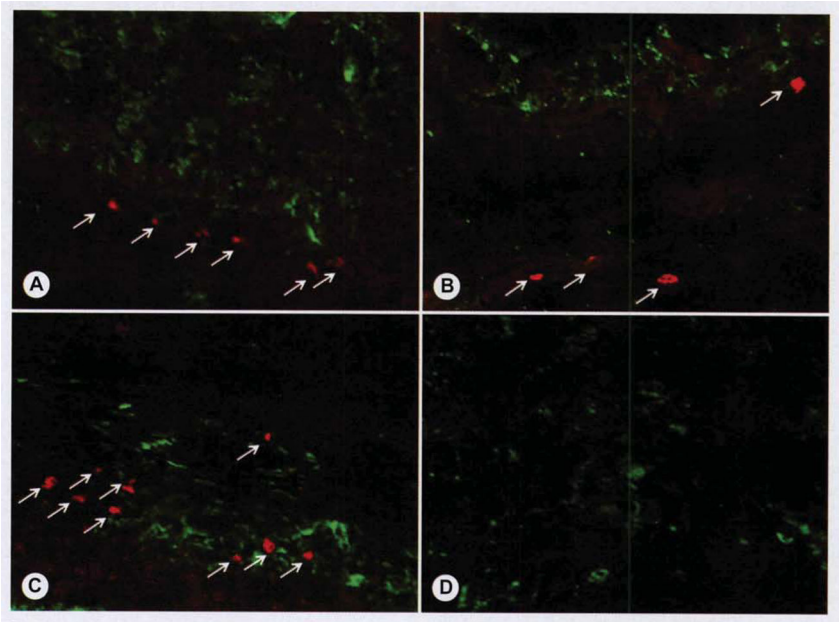

Fig. 5.

Motor end plates with neuronal contact. Immunohistochemical analysis was performed with fluorescent red secondary antibody to detect motor end plate–specific bungarotoxin, and fluorescent green secondary antibody was used to identify neuronal specific beta3-tubulin. **A**) MSC group demonstrated scattered areas of motor end plates (red; arrows) with scattered neuronal ingrowth (green) between myoblast cells. **B**) MT group demonstrated only rare motor end plates (red; arrows), and there was dense neuronal network (green) around myotubes. **C**) MEE group demonstrated both dense areas of motor end plates (red; arrows) throughout and dense neuronal infiltrate surrounding myotubes. **D**) PCL group, because of absence of tissue-engineered muscle on implant, failed to demonstrate motor end plates (red), although rare neuronal ingrowth (green) was detected within connective tissue adjacent to implant.

Author Manuscript Author Manuscript Author Manuscript Author Manuscript

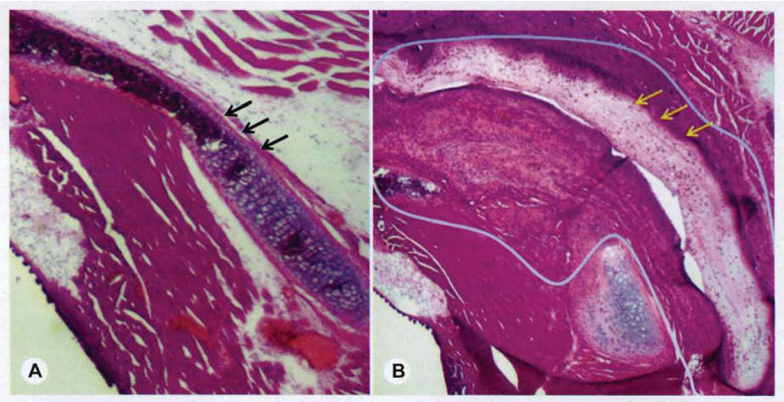

Fig. 6.

Muscle thickness (hematoxylin-eosin staining). **A**) Axial section of native rat larynx with thyroid cartilage intact (arrows). **B**) Section from MEE group at 1 month after implantation. Tissue-engineered muscle is outlined, and arrows demarcate polymer scaffold.

Author Manuscript Author Manuscript Author Manuscript Author Manuscript

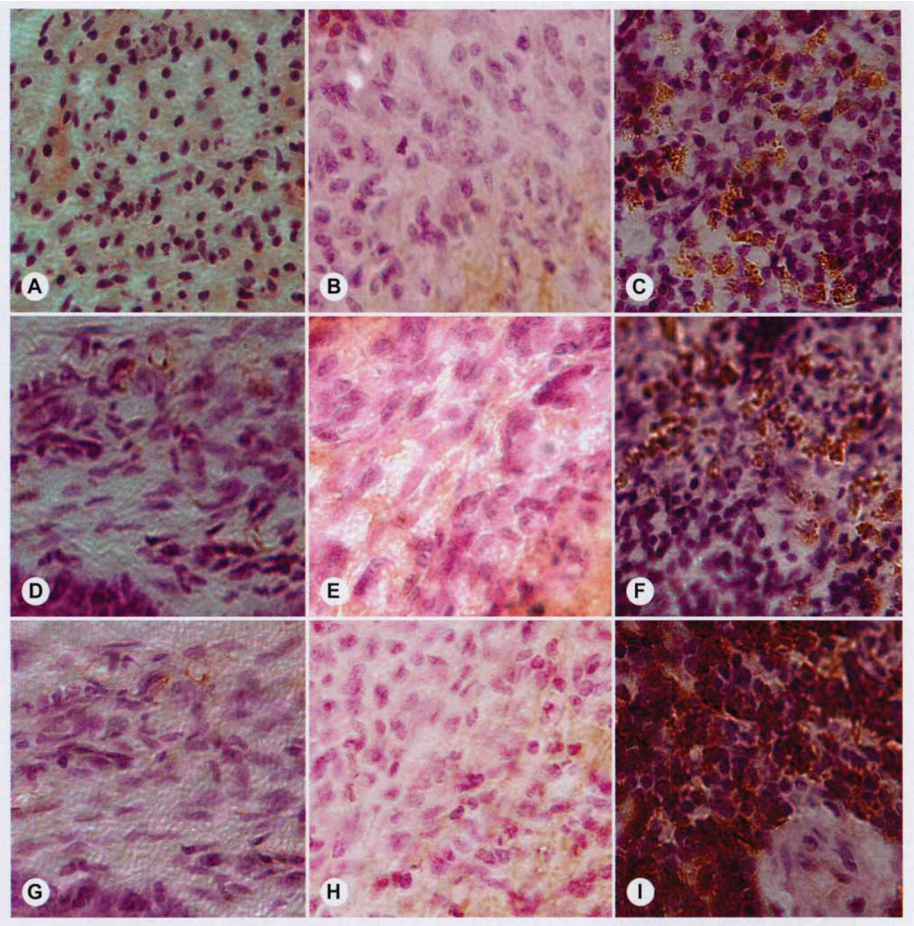

Fig. 7.

Inflammation and immunoreactivity. Although many implants demonstrated mild inflammatory infiltrate at surgical site, there was no evidence of immune-mediated rejection in any specimens. Rows represent anti-CD3 (**A–C**), anti-CD4 (**D–F**), and anti-CD8 (**G–I**) staining used to detect lymphocytes that mediate immune rejection. Left column (**A,D,G**) shows representative negative controls, middle column (**B,E,H**) shows representative study samples, and right column (**C,F,I**) shows positive controls (spleen). Fact that all study groups demonstrated absence of CD3, CD4, and CD8 lymphocytes suggests there was no specific rejection of tissue-engineered implants.

Author Manuscript

Author Manuscript

Author Manuscript

Author Manuscript

TABLE 1

MECHANICAL CHARACTERISTICS OF PCL IMPLANT IN COMPARISON TO NATIVE RAT CARTILAGE

	Native Rat Cartilage	PCL Implant Before Implantation
Maximum load (*N*)	1.61 ± 0.3	1.99 ± 0.3
Tensile strength (MPa)	1.57 ± 0.4	1.79 ± 0.3

PCL — poly(D,L-lactide-co-ε-caprolactone).

Author Manuscript Author Manuscript Author Manuscript Author Manuscript

TABLE 2

INNERVATION STATUS AND MUSCLE THICKNESS FOR EACH GROUP

	MSC Group	MT Group	MEE Group
Mean motor end plate count	82.6	44.3	87.3
Mean % of motor end plates with nerve contact	82.4%	65.8%	94.8%
Mean tissue-engineered muscle thickness (μm)	587.3	680.2	750.3

All data are based on review of 6 slides per animal.

MSC — muscle stem cell; MT — myotube; MEE — motor end plate–expressing. (See Partial Laryngectomy Procedures for further description of groups.)